Solution Conformations and Interactions of α and β Subunits of the *Oxytricha nova* Telomere Binding Protein: Investigation by Raman Spectroscopy†

Laurent Laporte, Julie Stultz, and George J. Thomas, Jr.*

Division of Cell Biology and Biophysics, School of Biological Sciences, University of Missouri−Kansas City, Kansas City, Missouri 64110

Received February 6, 1997; Revised Manuscript Received April 14, 1997⊗

ABSTRACT: Solution conformations of the α and β subunits of the *Oxytricha nova* telomere binding protein have been investigated by Raman spectroscopy. Raman spectra have also been obtained for a deletion mutant of the β subunit, βC232, which retains the N-terminal domain that is active in ternary complex (α:β:DNA) formation but lacks the C-terminal domain that is active in catalyzing guanine quadruplex formation. The Raman spectra show that α, β, and βC232 are rich in β-strand secondary structure (≈40−50%) and turns. The Raman signature of the C-terminal 153 amino acids of β, generated by subtracting the spectrum of βC232 (residues 1−232) from that of the full subunit, indicates that the domain active in guanine quadruplex formation contains less β-strand secondary structure and more irregular structure than the domain active in α:β:DNA formation. Raman markers also provide information about the environments and orientations of several key side chains, including tryptophan residues in N- and C-terminal domains of the β subunit. Both α and β denature between 30 and 40 °C, as evidenced by large changes in Raman bands diagnostic of main chain conformation and side chain environments. The Raman spectrum of an equimolar α/β mixture exhibits no evidence of specific interaction between the subunits; further, the denaturation profile of this mixture is indistinguishable from the sum of denaturation profiles of the constituent subunits, consistent with the absence of appreciable interaction between α and β throughout the range 0−50 °C. The present results provide insights into the solution conformations of the *Oxytricha* telomere binding protein subunits and serve as the basis for future study of subunit interactions with telomeric DNA.

Telomeres are the guanine-rich 3′ termini of eukaryotic chromosomes. In most organisms, the telomeric DNA strand consists of tandem repeats of the sequence $d(T_nA_mG_{3-4})$,[1] where *n* and *m* are small integers. These chromosomal ends are essential components of the cellular genetic machinery and are required specifically for accurate replication of the genome. Additionally, telomeres have been implicated in molecular mechanisms of aging, cancer, cell division, and chromosomal stability (Ashley & Wagenaar, 1974; Hastie et al., 1990; Hilliker & Appels, 1989; Lange et al., 1990; Lundblad & Szostak, 1989; Mandahl et al., 1985).

In many eukaryotes, the guanine-rich telomeric strand (3′) is longer than its complementary 5′ strand, resulting in a telomeric overhang. The overhang is protected by an as yet undetermined mechanism from endonuclease degradation that otherwise would compromise chromosomal integrity. Telomeres of several species have been found to participate in a protein−nucleic acid complex known as the telosome (Fang & Cech, 1995). This structure apparently provides the needed endonuclease protection (Gottschling & Zakian, 1986; Price & Cech, 1987). Recent experiments show that, despite involvement in the telosome complex, the telomeric DNA may still be available for elongation by telomerase and for replication (Shippen et al., 1994).

In the ciliated protozoan, *Oxytricha nova*, the telomeric DNA [sequence $d(T_4G_4)_2$] is bound by a heterodimeric protein. Analyses of the gene sequences and electrophoretic mobilities suggest that the larger α subunit has a molecular mass of 56 kDa, while the smaller and more highly basic β subunit has a molecular mass of 41 kDa (Gottschling & Zakian, 1986; Hicke et al., 1990; Gray et al., 1991). Both α and β are required for *in vitro* formation of a telomeric DNA−protein complex that exhibits the same guanine methylation protection patterns observed with *in vivo* preparations. The methylation pattern indicates that the telomere sequence, when bound by α and β (ternary complex), does not form the characteristic DNA quadruplex structures in which all guanines are associated via Hoogsteen hydrogen bonds (Gray et al., 1991). There is also evidence that the β subunit fulfills an additional function independent of the α subunit. In the absence of α, the β subunit promotes the formation of guanine quadruplexes *in vitro* (Fang & Cech, 1993a,b).

Interactions of the β subunit with telomeric DNA and with the α subunit have been probed using a deletion mutant, designated βC232 (Fang et al., 1993) that lacks the carboxy-terminal 153 amino acids. The truncated βC232 construct is capable of forming a ternary α:β:DNA complex with the same efficiency as the wild-type β subunit, but is apparently unable to induce the formation of guanine quadruplexes.

Here, we report the results of Raman spectroscopic investigations of the *Oxytricha* telomere-binding-protein subunits. We have probed the secondary structures of α, β, and βC232 and their interactions and thermostabilities in aqueous solutions.

† Part LXV in the series of papers on nucleic acids and nucleic acid-binding proteins. Supported by NIH Grant GM54378.

* Author to whom correspondence may be addressed.

⊗ Abstract published in *Advance ACS Abstracts,* June 15, 1997.

[1] Abbreviations: standard one-letter symbols (roman type) are employed for nucleotides and amino acids. Normal modes of vibration of the tryptophan and tyrosine residues are numbered in accordance with the notation of Takeuchi et al. (1986) and are printed in italic type.

S0006-2960(97)00283-3 CCC: $14.00 © 1997 American Chemical Society

MATERIALS AND METHODS

(1) Isolation and Purification of Subunits

The α and *β* subunits and the deletion mutant *β*C232 were expressed in *Escherichia coli* containing recombinant plasmid vectors generously provided by Dr. Thomas R. Cech of the University of Colorado. Proteins were extracted from the bacteria and purified using published procedures (Fang & Cech, 1993a,b).

Briefly, colonies of the *E. coli* host were grown at 37 °C on LB/agar plates containing tetracycline. Two single colonies were removed and each was placed in 20 mL of LB broth inoculated with 20 mL of tetracycline at 12.5 mg/mL and grown overnight at 37 °C in a thermostated shaker. Following the overnight growth, each 20 mL culture was placed in 2 L of LB media that was inoculated with 2 mL of tetracycline (12.5 mg/mL). The cultures were grown at 37 °C to an optical density (610 nm) in the range $0.8 < A_{610} < 1.2$, after which expression of the *Oxytricha* protein was induced by addition of 1 mL of 0.1 M isopropyl-1-thio-*β*-D-galactoside per liter of culture. The temperature was reduced to 30 °C and the cells allowed to grow an additional 4 h. The cells were harvested by centrifugation at 6000 rpm and 4 °C for 30 min, quick-frozen in liquid nitrogen, and stored at −80 °C for future use.

The expressed protein was recovered as needed by thawing and homogenizing the cells, adding 0.1 M phenylmethanesulfonyl fluoride and lysing by French press and sonication. The resulting mixture was centrifuged at 45 000 rpm and 4 °C for 1 h to pellet cell debris. The supernatant was removed, diluted with 150 mM HEND (50 mM HEPES buffer at pH 7.5, 1 mM EDTA, 150 mM NaCl, and 0.5 mM dithiothreitol) and applied to a CM-Sepharose column. Crude protein was eluted by the addition of 650 mM HEND. After elution, the crude protein solution was dialyzed extensively against 150 mM HEND, removed from the dialysis buffer and applied to an ISCO (Lincoln, NE) ProTeam column packed with SynChropak S300 strong cation exchanger. Subsequent elution against a linear salt gradient (from 0.15 to 1 M NaCl) yielded the purified protein, which was dialyzed first against 1 M TEND (10 mM Tris, pH 7.2, 1 mM EDTA, 1 M NaCl, and 0.5 mM dithiothreitol) and then against 50 mM TEND to provide the material used for spectroscopic analyses.

Typically, the preparation described above yielded milligram quantities of purified protein, varying from 4 mg for the *β*C232 mutant to approximately 30 mg for both the α and *β* subunits. Proteins were stored at −80 °C in a 50:50 vol % mixture of glycerol and 5 mM Tris buffer (pH 7.5), containing 0.5 mM EDTA and 50 mM NaCl. Prior to use, subunits were dialyzed extensively against the above 5 mM Tris buffer solution (hereafter referred to as sample buffer).

(2) Raman Spectroscopy

For Raman spectroscopy, α, *β*, and *β*C232 were prepared at approximately 50 mg/mL in sample buffer, using 30 and 10 kDa Centricons (Amicon, Beverly, MA). Both the α and *β* subunits were predominantly monomeric at concentrations employed for Raman spectroscopy as assayed by analytical ultracentrifugation (data not shown). Raman spectra were excited at 514.5 nm using 200 mW of radiant power from an Innova argon gas laser (Coherent, Inc., Santa Clara, CA) and were collected on a model 1877 Triplemate spectrograph (SPEX Industries, Metuchen, NJ) equipped with a liquid-nitrogen-cooled charge-coupled-device detector. Samples were maintained at constant temperature throughout each data collection protocol using a sample cell thermostat described previously (Thomas & Barylski, 1970).

RESULTS AND INTERPRETATION

(1) α Subunit

(a) Raman Spectrum and Assignments. The Raman spectrum of the α subunit of the *Oxytricha* telomere binding protein, dissolved to approximately 50 mg/mL in sample buffer at pH 7.2 and 10 °C, is shown in the top trace of Figure 1. Information regarding the protein secondary structure is contained in the Raman amide I band centered at 1667 cm^{-1} and amide III bands in the region 1230−1340 cm^{-1}. The basis for interperting these diagnostic amide bands has been discussed in recent reviews (Bandekar, 1992; Miura & Thomas, 1995). The central amide I peak at 1667 cm^{-1} is relatively sharp, indicating that *β*-strand is the dominant secondary structure. The partially resolved low-frequency shoulder near 1650 cm^{-1}, labeled with an arrow in the top trace of Figure 1, implies lesser amounts of α-helix and irregular conformations. This assessment is confirmed by the relatively high intensity of the amide III marker at 1242 cm^{-1} (*β*-strand plus irregular conformations) compared with amide III markers in the 1270−1300 cm^{-1} interval (α-helix conformation).

To estimate quantitatively the distribution of amide I intensity corresponding to different secondary structures, Fourier deconvolution was employed (Thomas & Agard, 1984). The results, shown in the top of Figure 2, suggest that the α subunit comprises at least 40−50% *β*-strand, and much smaller percentages of α-helix and irregular conformations. Application of the curve-fitting method of Berjot et al. (1987) to the amide I profile provides a similar estimate of *β*-strand (≈50%) (data not shown). The amide III profile of the α subunit in Figure 2 is consistent with the predominance of *β*-strand over other secondary structures. Circular dichroism measurements also indicate a low α-helical content for the α subunit (data not shown).

The three tryptophan residues of the α subunit (W147, W196, and W387) contribute to the Raman bands at 756, 880, 1008, 1340, 1360, and 1555 cm^{-1}. The broad band at 1555 cm^{-1}, which is assigned exclusively to normal mode *W3* of the indole ring (Takeuchi & Harada, 1986), is informative of the magnitude of the torsion $\chi^{2,1}$ (C2-C3-C*β*-Cα) of the average tryptophan side chain (Miura et al., 1989). Curve fitting and deconvolution procedures (data not shown) suggest that the broad 1555 cm^{-1} band comprises multiple components between 1551 and 1560 cm^{-1}, implying a distribution of tryptophan conformers with $|\chi^{2,1}|$ values between 95 and 120°. Information about indole N1H hydrogen bonding is obtained from the band corresponding to normal mode *W17*, expected in the range 875−882 cm^{-1} (Miura et al., 1988, 1991; Takeuchi & Harada, 1986). In the α subunit, the *W17* band is sharp and centered at 880 cm^{-1}, consistent with uniformly weak N1H hydrogen bonding for the three tryptophans per subunit.

The Raman band intensity ratio of the tyrosine Fermi doublet near 850 and 830 cm^{-1} (I_{850}/I_{830}) is diagnostic of phenoxyl hydrogen bonding (Siamwiza et al., 1975). The intensity ratio typically ranges between 0.30 for an OH group that is a strong hydrogen bond acceptor and 2.5 for an OH

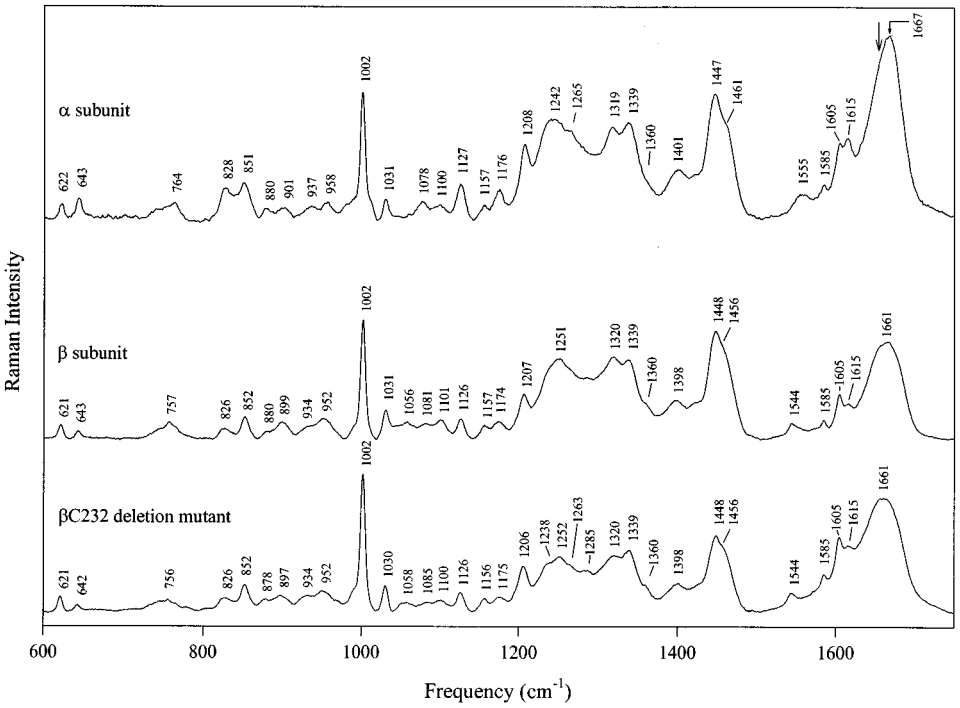

FIGURE 1: Raman spectra in the region 600−1750 cm^{-1} of the *Oxytricha* telomere binding protein. Top: α subunit. Middle: *β* subunit. Bottom: *β*C232 deletion mutant. Each spectrum was collected at 10 °C from a solution of the protein (approximately 50 mg/mL) in sample buffer containing 5 mM Tris (pH 7.2 ± 0.1), 0.5 mM EDTA, and 50 mM NaCl. The spectra were excited at 514.5 nm and corrected for contributions from the buffer and sloping baseline.

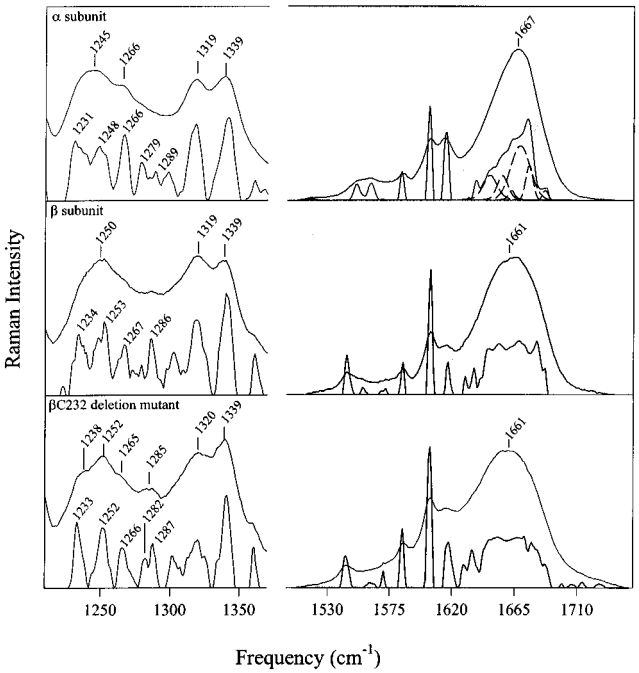

FIGURE 2: Fourier deconvolution of the regions of Raman amide III (1200−1350 cm^{-1}) and amide I (1600−1700 cm^{-1}) bands of the *Oxytricha* telomere binding protein. Top: α subunit. Middle: *β* subunit. Bottom: *β*C232 deletion mutant. Deconvolutions were obtained using a desmearing function of 22 cm^{-1} half-width (1000 cycles) according to the procedure of Thomas and Agard (1984). In the case of the α subunit, an additional 1000 cycles of deconvolution of the amide I complex allows separation of components at 1662, 1653, and 1645 cm^{-1} (dotted curve) with relative intensities of 0.44, 0.30, and 0.09, respectively, suggesting corresponding percentages of strand, irregular, and helix conformations. Analogous results (not shown) for the *β* subunit and *β*C232 deletion mutant are discussed in the text.

group that is a strong donor. Phenoxyls that are both donors and acceptors exhibit $I_{850}/I_{830} \cong 1.25$. From Figure 1, we find that $I_{850}/I_{830} = 1.1$ for the α subunit, indicating that the average phenoxyl (of 24 tyrosines) assumes both donor and acceptor roles at these experimental conditions.

The numerous glutamic (21) and aspartic acid residues (32) of the α subunit contribute to the broad and moderately intense band at 1401 cm^{-1}, diagnostic of the ionized carboxylate (CO_2^-) group (Fasman et al., 1978). The absence of a COOH Raman marker near 1700−1720 cm^{-1} confirms that all acidic side chains are ionized at the conditions employed.

Virtually all of the Raman bands of the α subunit can be assigned to specific vibrational modes of the peptide main chain or side chains, or to specific classes of amino acids, by reference to previously published work on proteins and model compounds. A comprehensive list of assignments is given in Table 1.

(b) Thermolability of Secondary Structure Assessed by Raman Spectroscopy.

Figure 3 shows the Raman spectrum of the α subunit as a function of temperature in the range 0−50 °C. No significant temperature dependence is detected between 0 and 30 °C; however, the spectrum changes dramatically between 30 and 40 °C, and further increases in temperature cause modest additional changes. Most striking is the narrowing of the amide I band above 30 °C, with little change in the band center (1666 cm^{-1}). Because *β*-strand secondary structure provides the greatest contribution to the amide I intensity in the interval 1665−1670 cm^{-1}, the observed change is interpreted as an increase in *β*-strand at the expense of other conformations. Consistent with this interpretation is the sharpening of the amide III band at 1235 cm^{-1}, which is the position expected for *β*-strand structure (Sargent et al., 1988). The difference spectra of Figure 3 also reveal that many side chain environments, including those of aromatic and aliphatic residues, are altered by thermal denaturation. We attribute the 50 °C spectrum of Figure 3 to a denatured form of the α subunit in which native

Table 1: Raman Bands and Assignments for *Oxytricha nova* Telomere Binding Protein Subunits[a]

α subunit		β subunit		βC232 fragment		
cm^{-1}	intensity	cm^{-1}	intensity	cm^{-1}	intensity	assignment
622	1.3	621	1.2	621	1.2	Phe (*F6b*)
643	1.7	643	0.6	642	0.4	Tyr (*Y6b*)
764	1.3	757	1.4	756	0.7	Trp (*W18*)
828	2.7	826	0.8	828	0.7	Tyr (*Y1* + *Y16a*)
851	3.0	852	1.9	852	1.7	Tyr (*Y1* + *Y16a*)
879	0.7	879	0.6	876	0.4	Trp (*W17*)
901	1.1	899	1.4	899	0.7	νCC
937	1.2	934	1.0	932	0.7	νCC
958	1.4	952	1.7	950	1.0	νCC
1002	10.0	1002	10.0	1002	10.0	Phe (*F12*)
1031	1.8	1031	2.4	1031	1.8	Phe (*F18a*)
		1056	1.5	1058	0.6	Lys, Glu
1078	1.5	1081	1.3	1085	0.6	νCC, νCN
1100	1.3	1101	1.6	1100	0.8	νCC, νCN, νCO
1127	2.9	1126	1.7	1126	1.4	Trp (*W13*)
1157	1.3	1157	1.2	1156	1.0	δCH_3
1176	2.1	1174	1.5	1176	1.1	Tyr (*Y9a*)
1208	6.0	1207	3.8	1206	3.4	Tyr (*Y7a*), Phe (*F7a*)
				1238	3.8 s	amide III, strand
1242	7.9					amide III, strand
		1251	6.7	1251	4.2	amide III, coil
1265	6.7 s			1263	3.7 s	amide III, helix
				1285	3.2	amide III, helix
1319	7.3	1320	6.9	1320	4.3	δCH_2
1339	7.7	1339	6.7	1339	4.7	δCH_2, Trp (*W7*)
1360	3.8	1360	2.9	1360	2.2	Trp (*W7*)
1401	4.0	1398	3.2	1400	2.2	symmetric νCO_2^-
1447	9.9	1448	9.0	1448	5.8	δCH_2
1461	7.6	1456	8.4	1456	8.7	δCH_3
1558	2.1	1544	1.4	1544	1.0	Trp (*W3*)
1585	2.9	1585	1.7	1585	1.4	Trp (*W2*), Phe (*F8b*)
1605	6.2	1605	3.8	1604	3.4	Tyr (*Y8b*), Phe (*F8a*)
1615	6.5	1616	3.0	1615	2.5	Tyr (*Y8a*), Trp (*W1*)
				1661	6.0	amide I
		1661	8.2			amide I
1667	14.6					amide I

[a] For each protein, Raman frequencies are in cm^{-1} units (first column), and intensities are on an arbitrary 0−10 scale (second column). Assignments, which are based upon previous studies, are discussed in the text. Abbreviations: s, shoulder, ν, stretching mode, δ, bending mode.

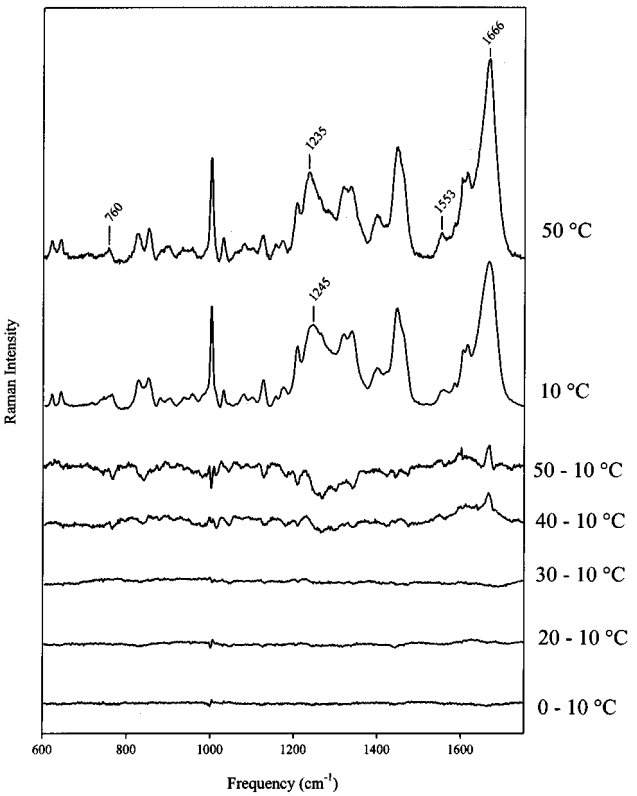

FIGURE 3: Thermostability of the α subunit of the *Oxytricha* telomere binding protein as monitored by Raman difference spectroscopy. The sample was prepared at approximately 50 mg/mL in sample buffer at pH 7.2. The spectra were maintained at the indicated temperatures throughout the data collection protocol. From top to bottom: α subunit at 50 °C; α subunit at 10 °C; difference spectra corresponding to 50−10, 40−10, 30−10, 20−10, and 0−10 °C. Labels indicate key bands that are discussed in the text. Spectra were corrected for background and solvent contributions.

conformations are replaced by non-native β-strand structure. Because solutions of the protein become highly opaque above 40 °C, thermal denaturation presumably involves extensive aggregation of subunits. We conclude that the native structure of the α subunit is highly thermolabile. The native fold is stable below 30 °C and denatures irreversibly above 30 °C.

(2) β Subunit

(a) Raman Spectrum and Assignments. The amide I and amide III bands of the β subunit are very broad in comparison to those of the α subunit (*cf.* top and middle traces of Figure 2), suggesting a broad distribution of secondary structure. Amide I and amide III deconvolutions (Figure 2) and curve-fitting results (data not shown) are consistent with this assessment.

The two tryptophans (W93 and W343) of the β subunit are expected to contribute a distinctive band corresponding to normal mode *W3* in the interval 1540−1560 cm^{-1}. In Figure 1, we observe a fairly sharp peak at 1544 cm^{-1} and a more diffuse shoulder at higher frequency. Deconvolution (not shown) locates the center of the shoulder at about 1553 cm^{-1}. These results imply that one tryptophan is characterized by a side chain torsion $|\chi^{2,1}| = 80°$, while the other tryptophan exhibits a range of $|\chi^{2,1}|$ values with an average near 100°. The tryptophan with $|\chi^{2,1}| = 80°$ is apparently located in a region of well-defined tertiary structure. Conversely, the tryptophan with $|\chi^{2,1}| > 80°$ may be located in a segment of the protein that lacks a well-defined tertiary structure. Although the data of Figure 1 do not indicate which tryptophan exhibits $|\chi^{2,1}| = 80°$, this value for the C2-C3-Cβ-Cα torsion is among the lowest observed in proteins and model compounds (Miura et al., 1989). Below, additional data are presented to suggest probable locations of the structurally distinguishable tryptophan side chains of the β subunit. (See Discussion and Conclusions section.) The *W17* marker (880 cm^{-1}) for the β subunit, like that for the α subunit, indicates that indole N1H groups are on average moderately hydrogen bonded.

The 13 tyrosines of the β subunit are characterized by $I_{850}/I_{830} = 2.3 \pm 0.1$ (Table 1), which implies that most phenoxyls exist as strong hydrogen bond acceptors (Siamwiza et al., 1975). This situation differs greatly from that observed for tyrosines of the α subunit. Other Raman markers of the β subunit are listed with assignments in Table 1.

(b) Thermostability. The temperature dependence of the Raman spectrum of the β subunit is displayed in Figure 4. The protein structure is essentially stable between 0 and 30 °C. However, upon heating to 40 °C, significant structural changes are evident. In particular, the enhancement of intensities of amide I and amide III bands (at 1668 and 1234 cm^{-1}, respectively) indicates the formation of additional β-strand at the expense of native secondary structure. At 50 °C, the solution becomes opaque and the amide markers

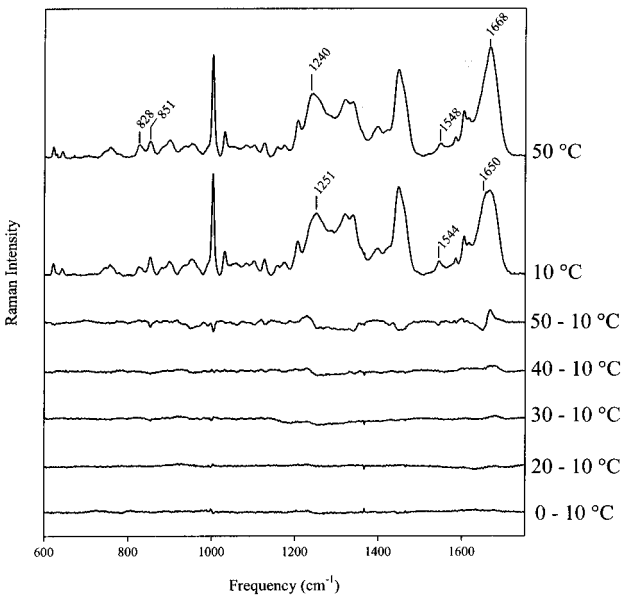

FIGURE 4: Thermostability of the β subunit of the *Oxytricha* telomere binding protein as monitored by Raman difference spectroscopy. Conditions are given in the Figure 3 legend.

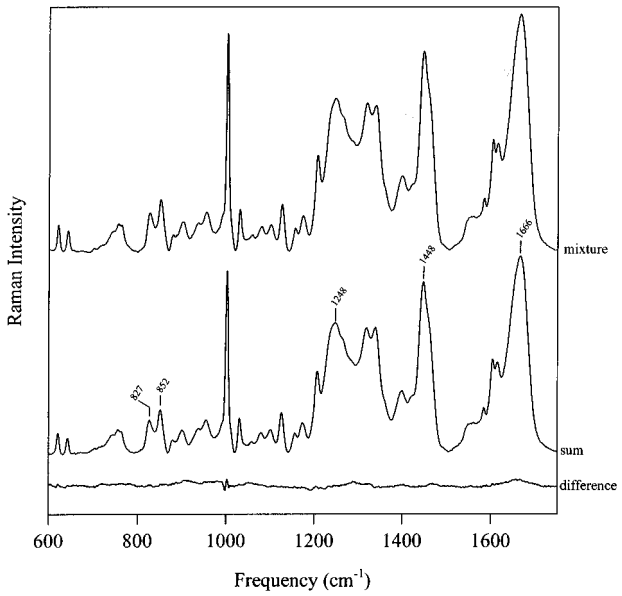

FIGURE 5: Comparison of the Raman spectrum of an equimolar mixture of α and β subunits (top trace) with the spectral sum of constituents (middle trace) at 10 °C. The difference spectrum (bottom trace), computed as mixture minus sum, is normalized to minimize the difference intensity of the sharp phenylalanine band near 1002 cm^{-1} in each spectrum. Other conditions are given in the Figure 3 legend.

are those of a predominantly β-stranded structure (Sargent et al., 1988). We conclude that thermal denaturation of the β subunit above 30 °C leads to extensive aggregation with β-strand formation. This is similar to the effect of thermal denaturation of the α subunit.

Difference bands attributable to aromatic residues are also observed in the 50-minus-10 °C difference spectrum of Figure 4. Upon heating from 10 to 50 °C, the intensity ratio (I_{850}/I_{830}) of the tyrosine Fermi doublet decreases from 2.4 to 1.2, indicating that tyrosines which are exclusive hydrogen bond acceptors in the native structure are converted to both donor and acceptor roles in the heat denatured structure. Such a conversion is consistent with exposure of tyrosine phenoxyl groups to solvent interactions. The complex Raman band corresponding to normal mode *W3* of tryptophans W93 and W343 exhibits a shift of its peak from approximately 1544 cm^{-1} at 10 °C to 1548 cm^{-1} at 50 °C, signaling a significant change in tryptophan indole orientations upon thermal denaturation. Figure 4 also shows that Raman markers, and therefore environments, of phenylalanyl and aliphatic side chains are altered by heat denaturation.

(3) βC232 Deletion Mutant: Raman Spectrum and Assignments

The βC232 deletion mutant lacks residues 233−385 of the wild-type β subunit. Interestingly, its Raman spectrum (Figure 1) is rather similar to that of the full β sequence, particularly with regard to the amide I profile, which consists of a very broad band at approximately 1661 cm^{-1}. Subtle differences in the amide I and amide III profiles of β and βC232 are revealed by their respective deconvolutions (Figure 2) or curve-fitted components (not shown). The deconvolutions of Figure 2, particularly those for the amide III interval, suggest that the ratio of β-strand to irregular structure is greater in βC232 than in the complete β subunit. The relative deficiency of non-β-strand structure in the truncated subunit implies that C-terminal residues 233−385 contain a greater proportion of non-β-secondary structure (turns, loops, etc.) than is present in residues 1−232.

The single tryptophan (W93) of βC232 exhibits its *W3* marker at 1544 cm^{-1}, implying that the tryptophan residue with $|\chi^{2,1}| = 80°$ in the native sequence (see above) is W93. This conclusion is based upon the assumption that the local structure and environment of residue W93 are similar in βC232 and in the native sequence. Accordingly, for residue W43, $|\chi^{2,1}| \approx 100°$.

The 11 tyrosines of the βC232 sequence appear to be largely unaltered in their phenoxyl hydrogen-bonding characteristics *vis-à-vis* the native sequence, as evidenced by the near invariance of I_{850}/I_{830} (=2.4). Thus, the tyrosine side chain environments and presumably also the tertiary structure of the N-terminus (residues 1−232) are not strongly coupled to the C-terminus (residues 233−385). Likewise, there are no apparent intensity differences between βC232 and β in the spectral regions 1400−1410 and 1700−1730 cm^{-1}, indicating that the eight fewer carboxylates (7D + 1E) of the former are unaffected by C-terminal truncation.

(4) Investigation of Interaction between α and β Subunits

Fang and Cech (1993c) investigated putative interaction between α and β subunits using UV cross-linking and denaturing gel electrophoresis. At the experimental conditions employed (<1 μM protein concentration), these authors concluded that α and β subunits do not interact appreciably with one another in the absence of DNA.

We have used Raman spectroscopy to investigate the possibility of interaction between α and β subunits at higher protein concentrations (>1 mM). In Figure 5, the solution Raman spectrum of an equimolar mixture of α and β is compared with the spectral sum of constituents. The computed difference (bottom trace) is a virtual null spectrum, indicating that neither frequency shifts nor intensity changes occur in Raman bands of α or β upon mixing the subunits at this concentration. In particular, the absence of difference bands in the amide I and amide III intervals confirms no appreciable change in secondary structure within the precision (±1%) of the amide band measurements. In addition, the barely detectable difference features that are observed (small frequency shift of the phenylalanine marker near 1002

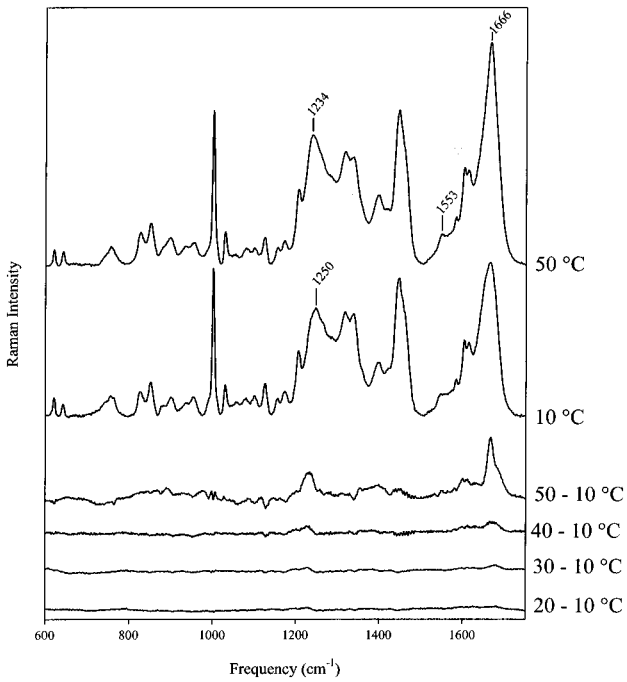

FIGURE 6: Thermostability of α and β subunits of the *Oxytricha* telomere binding protein in an equimolar mixture as monitored by Raman difference spectroscopy. The sample was prepared by mixing equal volumes of solutions of the two subunits, each at approximately 50 mg/mL in sample buffer at pH 7.2. Other conditions are given in the Figure 3 legend.

cm^{-1} and small intensity change of the aliphatic CH deformation marker near 1450 cm^{-1}) correspond to only the most intense Raman bands in the parent spectra and indicate that side chain environments, and therefore the subunit tertiary structures, are largely conserved in the mixture. This conclusion is consistent with our native PAGE analyses, which reveal only small changes in gel mobility of α and β in equimolar mixtures up to 70 mM concentration. The absence of significant Raman difference features in Figure 5 is consistent with the absence of interactions between α and β subunits (although interactions via rigid body interactions cannot be ruled out).

Figure 6 compares Raman spectra of an equimolar mixture of α and β subunits as a function of temperature between 10 and 50 °C. These results show that, in the mixture of α and β, the respective subunits exhibit the same thermolabilities evident in Figures 3 and 4. We conclude that the subunit thermostabilities are not altered in the equimolar mixture.

DISCUSSION AND CONCLUSIONS

Although the α and β subunits of the *Oxytricha* telomere binding protein have been extensively investigated using biochemical methods (Fang & Cech, 1993a; Fang et al., 1993; Gray et al., 1991; Hicke et al., 1990, 1994; Price & Cech, 1987), very little structural information at the molecular level is available. The present work provides a starting point for elucidating molecular structures and interactions of these telomere binding proteins.

C-terminal truncation of the β subunit at residue 232 does not eliminate its ability to form a ternary (α:β:DNA) complex (Fang & Cech, 1993a; Fang et al., 1993). However, βC232 is unable to promote the formation of parallel quadruplexes in guanine-rich telomeric DNA sequences tested for this activity by Fang and Cech (1993a). Conversely, N-terminal deletions (residues 1−122 and 1−192) eliminate ternary association activity, but retain the capability to promote

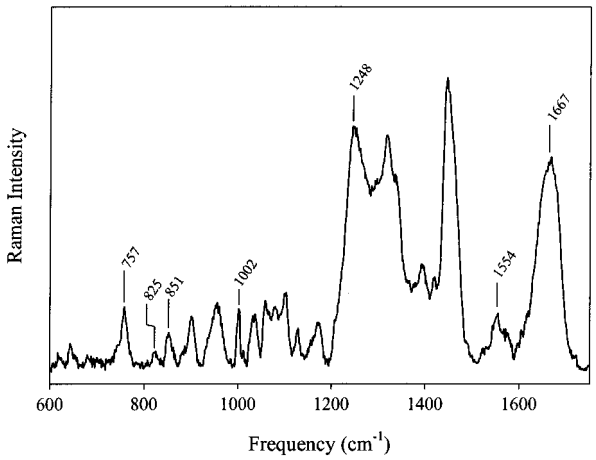

FIGURE 7: Raman spectrum of the C-terminal domain (residues 233−385) of the β subunit of the *Oxytricha* telomere binding protein. The spectrum was obtained by subtracting the spectrum of βC232 (Figure 1, bottom trace) from that of the β subunit (Figure 1, middle trace) using the phenylalanine peak at 1002 cm^{-1} as the intensity and frequency standard for spectral subtraction. The intensity that remains at 1002 cm^{-1} in this difference spectrum is due to the single phenylalanine residue (F337) in the C-terminal domain. Experimental conditions are given in the Figure 1 legend.

guanine quadruplexes (Fang et al., 1993). These results were interpreted by Cech and co-workers as evidence that the native β subunit comprises two functionally distinct domains, (i) the N-terminal domain, which is required for ternary association and (ii) the C-terminal domain, which is required for DNA quadruplex formation. Application of Raman difference spectroscopy to the present samples is expected to shed further light on this question. Specifically, subtraction of the spectrum of βC232 (N-terminal domain, Figure 1, bottom) from that of the full β subunit (Figure 1, middle) is expected to provide insight into structural features of the putative quadruplex forming domain (C-terminus).

Figure 7 shows the difference spectrum generated by subtraction of the Raman spectrum of βC232 from that of the full β subunit. This difference Raman spectrum is expected to approximate the Raman signature of the domain comprising residues 233−385, i.e., the domain active in guanine quadruplex formation. Interestingly, the resulting amide I and amide III profiles are similar in shape to those of the full β subunit. This is in accord with the conclusion reached above that secondary structures of the full protein and of the βC232 fragment (N-terminal domain, residues 1−232) are similarly rich in β-stranded structure and deficient in α-helix.

The difference spectrum of Figure 7 nevertheless displays an unusually broad amide I band, as well as an amide III band centered near 1250 cm^{-1}. Both of these features are characteristic of an irregular main chain conformation. This implies that the C-terminal domain is somewhat disordered. That the β domain putatively active in quadruplex formation comprises a disordered main chain is consistent with the recently determined crystal structure of another telomere binding protein, the yeast RAP1 protein (König et al., 1996). In RAP1, the C-terminus is thought to play a crucial role in DNA binding by wrapping around the major groove of the telomeric DNA duplex (Henry et al., 1990). A similarly unstructured element in the *Oxytricha* β subunit may be required for recognition of the telomeric repeat and for promotion of guanine quadruplex structures. The highly basic amino acid composition of the C-terminal domain

[residues 233−385 contain 38 lysines and 3 arginines (Gray et al., 1991)] is also consistent with a nucleic acid recognition motif (Harrison & Aggarwal, 1990; Pabo & Sauer, 1992).

In comparison to the β subunit, the α subunit is even richer in β-strand secondary structure. In fact, the Raman amide markers suggest very little α-helix structure in the α subunit (note the deep trough between 1265 and 1319 cm^{-1} in the amide III interval and the relatively narrow amide I band at 1667 cm^{-1} in the top trace of Figure 1).

We find no compelling evidence in Raman spectra (Figure 5) of specific interaction between α and β subunits. In particular, neither subunit conformations nor side chain environments are altered significantly in the α/β mixture, with the possible exception of a small net change in aliphatic side chain environments (1450 cm^{-1} marker). This is consistent with native gel studies of Fang and Cech (1993c), indicating the absence of α/β interactions in dilute sample preparations. Accordingly, we conclude that even at the higher concentrations employed here, α/β interactions do not occur or at least do not generate rearrangements of secondary structure and changes in side chain environments. Native gel electrophoresis of the same samples probed by Raman spectroscopy confirmed no appreciable interaction between α and β, in agreement with previous studies (Fang & Cech, 1993c).

Cech and co-workers demonstrated that both α and β subunits of the *Oxytricha* telomere binding protein can bind noncooperatively to telomeric DNA (Fang & Cech, 1993b; Fang et al., 1993). These binary complexes, α:DNA and β:DNA, exhibited different DNA methylation protection patterns. Additionally, the β subunit alone is sufficient to promote the formation of guanine quadruplexes, while the α subunit apparently is not. Both α:DNA and β:DNA are relatively unstable, as judged by association/dissociation kinetics (Fang et al., 1993). Conversely, the ternary complex (α:β:DNA) is formed cooperatively and is highly stable; yet, it exhibits no evidence of telomeric quadruplex formation. The α:β:DNA complex is also characterized by a DNA methylation protection pattern different from that of either α:DNA or β:DNA. The molecular basis of protein−DNA recognition in these binary and ternary complexes remains unresolved. Also unknown is the conformation of telomeric DNA in complexes with the telomere-binding-protein subunits. These and related structural issues can be addressed by Raman spectroscopy (Miura & Thomas, 1994; Miura et al., 1995). The present study has provided the Raman signatures of the *Oxytricha* telomere binding proteins in the absence of cognate DNA sequences. The results serve as the benchmark for subsequent study of telomeric protein−DNA complexes. The next paper of this series (Laporte & Thomas, 1997) will focus on (i) how the Raman signature of protein structure responds to recognition and binding of telomeric DNA and (ii) the conformation of telomeric DNA in complexes with telomere binding protein subunits.

ACKNOWLEDGMENT

Support of this research by the National Institutes of Health (Grant GM54378) and MMD-Scientific Education Partnership is gratefully acknowledged. We thank Professor Thomas R. Cech of the University of Colorado, Boulder, who generously provided plasmids and cells for expression of the *Oxytricha* telomere binding proteins. We also thank Dr. Guowei Fang of the Fred Hutchison Cancer Research Center, Seattle, Washington, for helpful discus-sions, and Dr. James M. Benevides for assistance in many phases of this work.

REFERENCES

Ashley, T., & Wagenaar, E. B. (1974) *Can. J. Genet. Cytol. 16*, 61−76.
Bandekar, J. (1992) *Biochim. Biophys. Acta 1120*, 123−143.
Berjot, M., Marx, J., & Alix, J. P. (1987) *J. Raman Spectrosc. 18*, 289−300.
Fang, G., & Cech, T. R. (1993a) *Cell 74*, 875−885.
Fang, G., & Cech, T. R. (1993b) *Biochemistry 32*, 11646−11657.
Fang, G., & Cech, T. R. (1993c) *Proc. Natl. Acad. Sci. U.S.A. 90*, 6056−6060.
Fang, G., & Cech, T. R. (1995) in *Telomeres* (Blackburn, E. H. & Greider, C. W., Eds.) pp 69−106, Cold Spring Harbor Laboratory Press, Plainview, New York.
Fang, G., Gray, J. T., & Cech, T. R. (1993) *Genes Dev. 7*, 870−882.
Fasman, G., Itoh, K., Liu, C. S., & Lord, R. C. (1978) *Biopolymers 17*, 1729−1746.
Gottschling, D. E., & Zakian, V. A. (1986) *Cell 47*, 195−205.
Gray, J. T., Celander, D. W., Price, C. M., & Cech, T. R. (1991) *Cell 67*, 807−814.
Harrison, S. C., & Aggarwal, A. K. (1990) *Annu. Rev. Biochem. 59*, 933−969.
Hastie, N. D., Dempster, M., Dunlop, M. G., Thompson, A. M., Green, D. K., & Allshire, R. C. (1990) *Nature 346*, 866−868.
Henry, Y. A. L., Chambers, A., Tsang, J. S. H., Kingsman, A. J., & Kingsman, S. M. (1990) *Nucleic Acids Res. 18*, 2617−2623.
Hicke, B. J., Celander, D. W., MacDonald, G. H., Price, C. M., & Cech, T. R. (1990) *Proc. Natl. Acad. Sci. U.S.A. 87*, 1481−1485.
Hicke, B. J., Willis, M. C., Koch, T. H., & Cech, T. R. (1994) *Biochemistry 33*, 3364−3373.
Hilliker, A. J., & Appels, R. (1989) *Exp. Cell. Res. 185*, 297−318.
König, P., Giraldo, R., Chapman, L., & Rhodes, D. (1996) *Cell 85*, 125−136.
Lange, T. D., Shiue, L., Myers, R. M., Cox, D. R., Naylor, S. L., Killery, A. M., & Varmus, H. E. (1990) *Mol. Cell. Biol. 10*, 518−527.
Laporte, L. & Thomas, G. J., Jr. (1997) (manuscript in preparation).
Lundblad, V., & Szostak, J. W. (1989) *Cell 57*, 633−643.
Mandahl, N., Heim, S., Kristoffersson, U., Mitelman, F., Rooser, B., Rydholm, A., & Willen, H. (1985) *Hum. Genet. 71*, 321−324.
Miura, T., & Thomas, G. J., Jr. (1994) *Biochemistry 33*, 7848−7856.
Miura, T., & Thomas, G. J., Jr. (1995) in *Subcellular Biochemistry* (Biswas, B. B., & Roy, S., Eds.) Vol. 24, pp 55−99, Plenum Press, New York.
Miura, T., Takeuchi, H., & Harada, I. (1988) *Biochemistry 27*, 88−94.
Miura, T., Takeuchi, H., & Harada, I. (1989) *J. Raman Spectrosc. 20*, 667−671.
Miura, T., Takeuchi, H., & Harada, I. (1991) *Biochemistry 30*, 6074−6080.
Miura, T., Benevides, J. M., & Thomas, G. J., Jr. (1995) *J. Mol. Biol. 248*, 233−238.
Pabo, C. O., & Sauer, R. (1992) *Annu. Rev. Biochem. 61*, 1053−1095.
Price, C. M., & Cech, T. R. (1987) *Genes Dev. 1*, 783−793.
Sargent, D., Benevides, J. M., Yu, M.-H., King, J., & Thomas, G. J., Jr. (1988) *J. Mol. Biol. 199*, 491−502.
Shippen, D. E., Blackburn, E. H., & Price, C. M. (1994) *Proc. Natl. Acad. Sci. U.S.A. 91*, 405−409.
Siamwiza, M. N., Lord, R. C., Chen, M. C., Takamatsu, T., Harada, I., Matsuura, H., & Shimanouchi, T. (1975) *Biochemistry 14*, 4870−4876.
Takeuchi, H., & Harada, I. (1986) *Spectrochim. Acta 42A*, 1069−1078.
Thomas, G. J., Jr., & Agard, D. A. (1984) *Biophys. J. 46*, 763−768.
Thomas, G. J., Jr., & Barylski, J. R. (1970) *Appl. Spectrosc. 24*, 463−464.

BI970283G